Optical Engineering

SPIEDigitalLibrary.org/oe

Uncooled long-wave infrared small pixel focal plane array and system challenges

Dieter Lohrmann
Roy Littleton
Colin Reese
Dan Murphy
Jay Vizgaitis

Downloaded From: http://spiedigitallibrary.org/ on 05/08/2013 Terms of Use: http://spiedl.org/terms

Report Documentation Page

Form Approved
OMB No. 0704-0188

Public reporting burden for the collection of information is estimated to average 1 hour per response, including the time for reviewing instructions, searching existing data sources, gathering and maintaining the data needed, and completing and reviewing the collection of information. Send comments regarding this burden estimate or any other aspect of this collection of information, including suggestions for reducing this burden, to Washington Headquarters Services, Directorate for Information Operations and Reports, 1215 Jefferson Davis Highway, Suite 1204, Arlington VA 22202-4302. Respondents should be aware that notwithstanding any other provision of law, no person shall be subject to a penalty for failing to comply with a collection of information if it does not display a currently valid OMB control number.

1. REPORT DATE	2. REPORT TYPE	3. DATES COVERED
JAN 2013		**00-00-2013 to 00-00-2013**

4. TITLE AND SUBTITLE	5a. CONTRACT NUMBER
Uncooled long-wave infrared small pixel focal plane array and system challenges	5b. GRANT NUMBER
	5c. PROGRAM ELEMENT NUMBER
6. AUTHOR(S)	5d. PROJECT NUMBER
	5e. TASK NUMBER
	5f. WORK UNIT NUMBER
7. PERFORMING ORGANIZATION NAME(S) AND ADDRESS(ES) **US Army RDECOM CERDEC NVESD,Ft. Belvoir,VA,22060**	8. PERFORMING ORGANIZATION REPORT NUMBER
9. SPONSORING/MONITORING AGENCY NAME(S) AND ADDRESS(ES)	10. SPONSOR/MONITOR'S ACRONYM(S)
	11. SPONSOR/MONITOR'S REPORT NUMBER(S)

12. DISTRIBUTION/AVAILABILITY STATEMENT
Approved for public release; distribution unlimited

13. SUPPLEMENTARY NOTES
Optical Engineering 52(6), 061305 (June 2013)

14. ABSTRACT

15. SUBJECT TERMS

16. SECURITY CLASSIFICATION OF:			17. LIMITATION OF ABSTRACT	18. NUMBER OF PAGES	19a. NAME OF RESPONSIBLE PERSON
a. REPORT	b. ABSTRACT	c. THIS PAGE			
unclassified	**unclassified**	**unclassified**	**Same as Report (SAR)**	**8**	

Uncooled long-wave infrared small pixel focal plane array and system challenges

Dieter Lohrmann
Roy Littleton
Colin Reese
Dan Murphy
Jay Vizgaitis
US Army RDECOM CERDEC NVESD
Ft. Belvoir, Virginia 22060
E-mail: dieter.j.lohrmann.civ@mail.mil

Abstract. There is a strong motivation for smaller pixels based on end-user demand for lower-cost, higher-resolution camera systems both for military and commercial applications. Uncooled detector technology fits the need for a low size, weight, and power system. We explore the trade-offs and challenges to achieving pixel designs smaller than the current 17-μm state-of-the-art detectors without loss in sensitivity or resolution. For illustration we consider a 12-μm design. We also address modulation transfer function issues as the pixel size shrinks, and examine the difference between the performance of present devices and the theoretical performance limit for uncooled detectors. © *The Authors. Published by SPIE under a Creative Commons Attribution 3.0 Unported License. Distribution or reproduction of this work in whole or in part requires full attribution of the original publication, including its DOI.* [DOI: 10.1117/1.OE.52.6.061305]

Subject terms: uncooled; bolometer; infrared detector; focal plane arrays; infrared imaging.

Paper 121416SS received Oct. 1, 2012; revised manuscript received Dec. 5, 2012; accepted for publication Dec. 7, 2012; published online Jan. 31, 2013.

1 Introduction

Fifteen to 20 years ago, developments in the semiconductor industry enabled the earlier generations of uncooled focal plane array (FPAs) and cameras with small format, 160 by 120 and then 320 by 240 array sizes with large pixels, generally in the neighborhood of 50×50 μm^2. The detector material was usually vanadium oxide (VOx), alpha-silicon (a-Si) or ferroelectrics. The wave band over which the optics and detectors of a camera were generally designed to receive and respond to radiation that is approximately $7.5 \pm .0.5$ μm^2 to 13 ± 1 μm^2. The user community, mainly the military at that time, specified camera operational requirements, which were typically around a 50-mK noise equivalent temperature difference (NETD), a frame rate of 30 Hz, and commensurate time constants for applications such as a thermal weapons sight or helmet-mounted goggles. The sensitivity of the detectors was far from the fundamental limits and thus drove the need for optics with an F/number near 1.0 to obtain the desired NETD. The modulation transfer function (MTF) of the system was almost never dominated by the MTF of the optics. Over the years, the semiconductor industry has made advances with ever smaller design rules, enabling the uncooled camera manufacturers to further push their designs and performance. Pixel sizes have been reduced from 50 to ~25 μm, then to 17 μm, and today uncooled camera manufacturers are looking into developing FPAs with pixels in the range of 10 to 13 μm while also increasing the resolution of the arrays to a nominal 1 K $\times$ 1 K format.[1,2] The user-desired operational specifications generally require a 35- to 50-mK NETD and a 10- to 12-ms time constant with a frame rate of 30 or 60 Hz. A nominal F/1 optic is still required to obtain this sensitivity. There is also interest in further shortening the time constant to 5 ms or less while maintaining good NETD performance for higher speed motion applications. This raises a number of considerations, practical and theoretical, related to the benefits of making uncooled detector pixels much smaller than 17 μm. This paper explores some of those considerations.

2 System MTF Constraints

The overall system MTF consists of a number of contributors including optics, detector (size, shape, fill factor, etc), electronics, motion blur, display, eye, vibration, and atmosphere. For this analysis, the concept of the system MTF is reduced to the sensor side of the system and comprised of the optics and the detector to identify the theoretical limits of an uncooled system. The other components are necessary to translate the theoretical system to a practical system. Here we consider only circular optics and square detectors. Changing these shapes does not change the argument; it merely slightly shifts it. The exception is a system with a highly obscured aperture[3] that can have a substantial change in the shape of an MTF curve. For a circular aperture, the optics diffraction MTF curve is described by the following equation, where ρ_c is the optics cutoff frequency described by $\rho_c = 1/\lambda F$. Here λ is the wavelength and F is the F/number.

$$\mathrm{MTF}_{\mathrm{optics}}(\rho) = \frac{2}{\pi}\left[\cos^{-1}\left(\frac{\rho}{\rho_c}\right) - \frac{\rho}{\rho_c}\sqrt{1-\left(\frac{\rho}{\rho_c}\right)^2}\right]$$

The detector MTF for a square pixel is below where a is the instantaneous field of view (IFOV) and $a = d/f$. Here d is the pixel width, f is the focal length, and u is the spatial frequency.

$$\mathrm{MTF}_{\mathrm{detector}}(u) = \sin\, c(\pi a u)$$

The "system" MTF as described by just the optics and detector is then the multiplication of the optics MTF and the detector MTF.

$$\mathrm{MTF}_{\mathrm{system}} = \mathrm{MTF}_{\mathrm{optics}} \times \mathrm{MTF}_{\mathrm{detector}}$$

The ideal detector MTF is dependent solely on the detector size, while the diffraction optics MTF is dependent on

Downloaded From: http://spiedigitallibrary.org/ on 05/08/2013 Terms of Use: http://spiedl.org/terms

the F/number and the wavelength. These dependencies are why the relationship between the optics and detector is often described by the ratio $F\lambda/d$. This figure of merit can then be used to describe the regions where a system is described as diffraction limited and where the system is considered detector limited, as done by Driggers.[4] If we consider the optics cutoff frequency (ρ_c), the detector cutoff frequency ($u_c = 1/d$), and the Nyquist frequency $[1/(2u_c)]$, three different optics MTF curves can be calculated to identify these regions of interest. Setting the optics cutoff to have zero MTF at the Nyquist frequency results in an $F\lambda d = 2$. Setting the diffraction based optics blur to equal the detector pixel size results in an $F\lambda d = 0.41$. These two curves generate the regions of the system that are described as "optics limited" and "detector limited." Driggers also describes a transition region between these two curves.[4] This transition region can be further split by setting the optics cutoff frequency to equal the detector cutoff frequency, resulting in an $F\lambda d = 1.0$. The region that lies between the diffraction limited and this curve can be further described as being "optics dominated," while the region between this curve and the detector limited curve can be described as being "detector dominated." In the optics-dominated region, changes to the optics have a greater impact on the system MTF than the detector. Likewise for the detector dominated region. These curves are described in Fig. 1 for the optics and detector MTF and in Fig. 2 for the "system" MTF.

It is educational to look at the results of the $F\lambda/d$ relationships in the terms of diffraction spot sizes, and relate them to the size of the pixel. Using the Rayleigh spot size formula, $B_{\text{lur}} = 2.44 * \lambda * F$, when $F\lambda d = 0.41$, the spot size equals the size of the pixel. When $F\lambda d = 1.0$, the spot size equals 2.44 times the size of the pixel, and likewise, when $F\lambda d = 2.0$, the spot size equals 4.88 times the size of the pixel. The relationship for these values and other pixel sizes (historic and potential future) are described in Table 1.

Table 1 and Figs. 1 and 2 highlight a few very key points for trying to determine what the smallest practical reasonable size is for a an uncooled FPA. The motivation for decreasing the pixel size is to enable smaller, lighter optics for a given

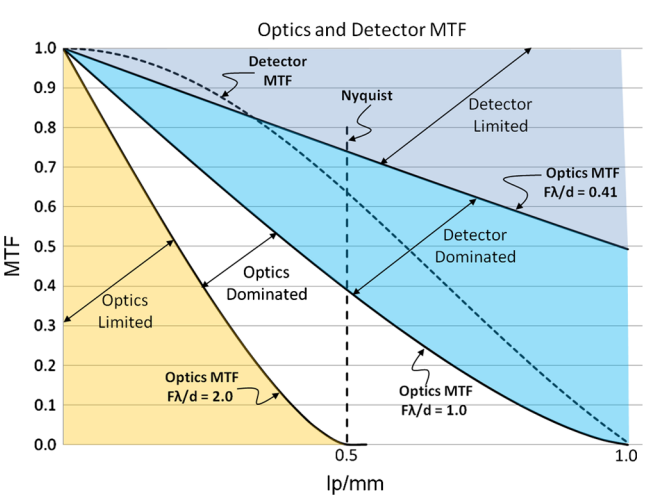

Fig. 1 Optics modulation transfer function (MTF) and detector MTF curves for various $F\lambda/d$ conditions describing the different regions within the design space. Spatial frequencies are normalized to the detector cutoff.

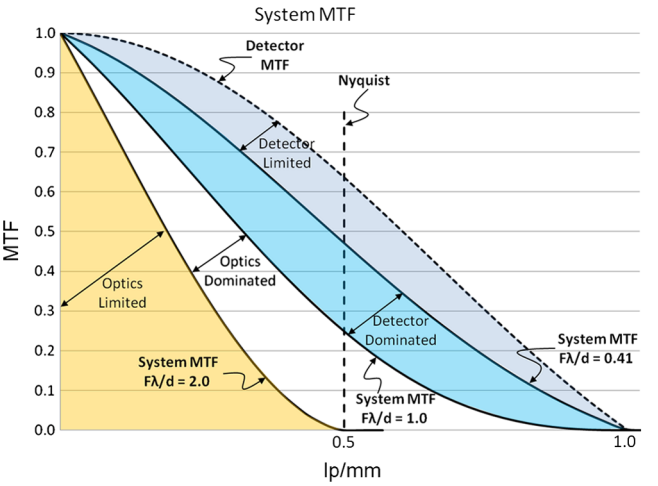

Fig. 2 System MTF curves further illustrating the different regions within the design space for various $F\lambda/d$ conditions. Spatial frequencies are normalized to the detector cutoff.

FOV if NETD remains constant. The optics volume is reduced in terms of focal length and diameter, which translates to reduced size and weight. However, going to smaller pixel sizes increases the $F\lambda/d$ value for any given F/number. If we design the system to the absolute resolution limit ($F\lambda d = 2$), then the smallest pixel for a 10-μm center wavelength would be 5 μm based on F/1.0 optics.

In uncooled systems, sensitivity often drives the designs more than resolution, driving the F/number to values between 1 and 1.4. Since sensitivity is inversely proportional to F^2, uncooled pixel technology has to continually become more sensitive in order to maintain a reasonable F/number. Assuming a fundamental limitation in the sensitivity of a pixel, there will become a point at which our spot sizes will become too large to provide a reasonable sensitivity for the FPA. Historically, most systems have been designed to have a resulting optics blur (to include aberrations) of less than 2.5 pixels ($\sim F\lambda/d < 1.0$). This is of course very dependent on the application and range requirements. Figure 3 illustrates the diffraction MTF curve of a lens for a 12-μm pixel at F/1.2 as compared to modeled optics designs from larger pixels. In this case, the IFOV remained constant by scaling the focal length and aperture with the pixel size (thus a single detector MTF for the three systems when observed in object space). The aberrated MTF curves for the 25 and 17-μm pixel designs still remain above the diffraction limit for the 12-μm optics with the same IFOV and F/number (including aberrations and tolerances). If an equivalent performance is desired from a smaller pixel, a similar MTF is required. In this case, a 12-μm pixel would require the equivalent of diffraction limited MTF curve at F/1.2, or roughly the equivalent of performance associated with $F\lambda d = 1.0$ to maintain the same performance. Since this is the transition point to the optics-dominated region, any further degradation to the optics via aberrations or tolerances has a more significant impact to the system performance, making the optics more of a challenge as the pixel size shrinks. In this case, a 12-μm pixel with optics at f/1.2 would be required to have zero degradation from the diffraction limit to maintain the same performance as the larger pixel systems. In order to obtain the advantage of small pixels, the fabricated optics is

Downloaded From: http://spiedigitallibrary.org/ on 05/08/2013 Terms of Use: http://spiedl.org/terms

Table 1 Calculations for F/number, spatial frequencies, and spot sizes for various $F\lambda/d$ conditions and pixel sizes. $F/ \geq 1.0$ for practical optics.

$\lambda = 10\ \mu$m	F/number			Detector		Diffraction spot size		
Pixel size (μm)	$F\lambda/d = .41$	$F\lambda/d = 1.0$	$F\lambda/d = 2.0$	Nyquist (lp/mm)	Cutoff (lp/mm)	$F\lambda/d = .41$ (μm)	$F\lambda/d = 1.0$ (μm)	$F\lambda/d = 2.0$ (μm)
50	2.05	5.0	10.0	10	20	50	122	244
25	1.02	2.5	5.0	20	40	25	61	122
17	0.70	1.7	3.4	29.4	58.8	17	41.5	83
12	0.49	1.2	2.4	41.7	83.3	12	29.3	58.6
10	0.41	1.0	2.0	50	100	10	24.4	48.8
8	0.33	0.8	1.6	62.5	125	8	14.6	29.2
6	0.25	0.6	1.2	83.3	167	6	14.6	29.2
5	0.2	0.5	1.0	100	200	5	12.2	24.4

required to be closer to the diffraction limit. Selecting pixel sizes that enable systems to be designed outside of the optics-dominated region allow for more leniencies on the optics design and tolerance.

Current uncooled systems are generally designed at $F\lambda/d \leq 1.0$. While the $F\lambda d = 2.0$ MTF curve is useful to generate the spatial resolution limits based on diffraction, many applications are not solely limited by resolution, and require an $F\lambda d = 1.0$. This is useful knowledge in determining the practical limit in pixel size. Assuming that optics faster than f/1.0 are not very practical, it is easy to see from Table 1 that 10 μm may be the most practical minimum pixel size to select. Systems that can benefit from an MTF curve at $F\lambda d = 2.0$ (resulting in smaller optics) can still be designed via a slower F/number up to f/2.0. Systems that required more MTF (such as $F\lambda d = 1.0$) are still feasible. If 5 μm was selected as a practical minimum pixel, the flexibility to design the system at anything other than $F\lambda d = 2.0$ is gone. This would significantly limit the performance capability for a number of applications for uncooled systems. This flexibility is crucial in determining the practical limitations of the pixel size.

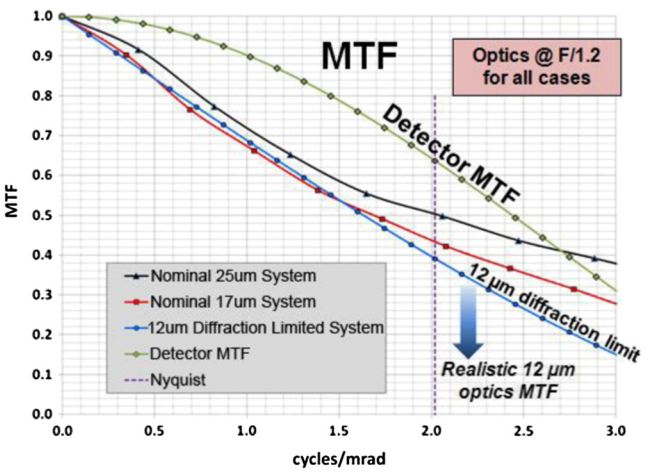

Fig. 3 Optics and detector MTF curves for 12-, 17-, and 25-μm pixel systems showing the aberrated curves from the larger pixels falling slightly higher than the $F\lambda d = 1.0$ condition for the 12-μm pixel system.

3 Limiting Factors for Performance of Small Pixel Microbolometers

The small pixel microbolometer development started with the ~25-μm pixel (circa 2001)[5] that provided a multi layer structure that separated the thermal isolation from the optical fill factor for improved sensitivity. Continued improvements in photolithography and transitioning from projection aligners to 150 mm steppers with line width resolution improving from 2 μm to 0.5 μm (2004–2010) have been sufficient for fabricating the current detector products. Detector designs in the 10- to 13-μm range will require deep ultraviolet (UV) photolithography with line widths <0.25 μm (2012 to 2014). The combination of uncooled detector designs and processes have allowed significant advancements in performance improvements and yields; Hence, uncooled has become the technology of choice for low-cost, high-performance systems with reduced size, weight, and power (SWaP). The latest improvement is the transition from 150-mm in-house wafer production facilities to commercial CMOS/MEMS (class1) foundries[6] with low defect, high yield, and 200-mm

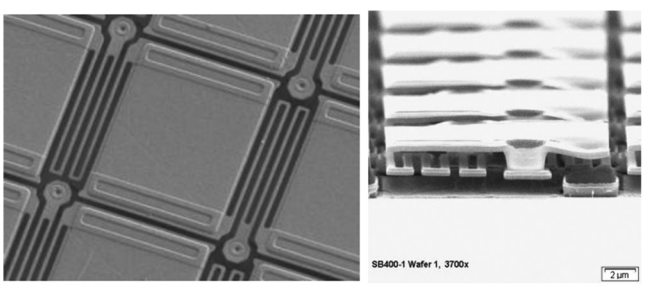

(a) Single level design (b) Multiple level design

Fig. 4 SEMs of 17-μm bolometer pixels with fine line geometry for (a) single- and (b) multiple-level pixel designs.

Downloaded From: http://spiedigitallibrary.org/ on 05/08/2013 Terms of Use: http://spiedl.org/terms

high-volume wafer capability. Figure 4 is an example SEM of foundry-processed bolometer with leg widths of <0.0.2 μm for single-level and multi-level designs.[7–9]

There is, however, a significant design and process challenge for microbolometer designs <17 μm. Specifically, with as much as a 15× to 25× reduction in pixel area from the initial 50-μm designs, there is a proportional increase in NETD (Sec. 4) unless significant design changes are made for pixels in the range of 12 μm (a notional design for illustration), and even more so for 5-μm pixels. This design requires a significant decrease in thermal conductance, such as decreasing leg width and thickness or an increase in leg length to maintain sensitivity while thinning the bridge for lower mass to reduce or maintain a reasonable time constant. Figure 5 shows actual SEMs for bolometer pixels of 50-, 25-, and 17-μm designs with approximate area scaling added for a notional 12-μm design. This figure clearly demonstrates the area challenges when the pixel size is reduced from 50 μm to notionally 12 μm and the importance of having a fine-line photolithography capability to make the desired changes stated above.

4 Design Considerations and Practical Limits

The theory below provides a roadmap of design considerations and tradeoffs that need to be addressed for all bolometer pixel designs especially as the pixel area is decreased. The basic equation for a typical VOx detector and its NETD is given as[10–12]

$$\Delta T_{\mathrm{NeTD}} \approx \gamma \Delta T_{\mathrm{TF}} \sqrt{1 + \frac{2}{\alpha^2 T_{\mathrm{sub}} \Delta T_r} + \frac{C_{\mathrm{th}}}{kT_{\mathrm{sub}}^2} \frac{\chi^2}{\alpha^2} B_{1/f} + \ldots}$$

$$\Delta T_{\mathrm{TF}} = \sqrt{\frac{kT_{\mathrm{sub}}^2}{C_{\mathrm{th}}}} \quad \gamma \equiv \frac{G}{\eta \frac{1}{4F^2+1} A_D \frac{dP_b}{dT_b}},$$

where T_{sub} is the substrate temperature over which the VOx detector is suspended and is taken as 300 K, α is the temperature coefficient of resistance (hereafter TCR), ΔT_r is the temperature change caused by the applied bias pulse, η is the fraction of power absorbed in the detector from the incoming radiation appearing at the lens surface, C_{th} is the detector heat capacity (J/K), G is the thermal conductance (W/K) between the detector and its surroundings, A_D is the pixel area (cm^2), dP_b/dT_b is the ideal blackbody power radiated between the band admitted through the lens and for 8 to 12 μm is 1.98×10^{-4} W/cm^2 K, $B_{1/f}$ is the integral over all frequencies of the $1/f$ noise spectrum multiplied by the magnitude squared of the readout electronics transfer functions, χ is the $1/f$ noise factor (the product $B_{1/f}$ and χ is dimensionless), F is the optic F/number, and k is Boltzmann's constant. The band 8 to 12 μm is chosen as a reference band for computational purposes. It also provides a benchmark for normalization purposes, as the actual band varies from manufacturer to manufacturer.

The temperature fluctuation term ΔT_{TF} represents the noise remaining when all the terms under the radical are small compared to one. It represents the noise due to the exchange of heat between the detector and its surroundings through the thermal conductance of the legs suspending the detector over the substrate and also the radiation conductance of the detector with its surroundings, including the scene seen through the lens. Due to a combination of cost and practical limitations of the lithography tools available to manufacture suspended structures, the thermal conductance of the legs is presently much larger than the radiation conductance for smaller pixels at this time. Thus, we are still far from the fundamental limits of performance at which typically cooled detectors operate.

It is not practical to make all of the noise terms fully negligible compared to the temperature fluctuation noise. In practice, the second term representing the electrical Johnson noise contribution of the detector often requires a considerable electric bias pulse be applied. Many designs target this term to be about one or equal to the temperature fluctuation noise. For typical TCR values of 2.5%, the bias-induced temperature change on the detector would need to exceed 10°C. However, for bias-induced temperature changes at this level and larger, the simple approximations for NETD begin to break down.[10] The third term represents $1/f$ noise of the detector, which increases as the detectors become smaller. To the extent it becomes a problem, materials research work becomes necessary to figure out how to lower the $1/f$ noise factor constant (χ), since it depends on volume and material properties. This term, along with additional downstream noise introduced by the readout electronics, is generally thought not to exceed the total noise by more than twice the temperature fluctuation noise.

Further design constraints are a 10-ms second time constant for an approximate match for a 30-Hz (or 60-Hz) video frame rate, and maintaining a sensitivity of ~35 mK as we reduce the pixel size. With the total noise set at about two

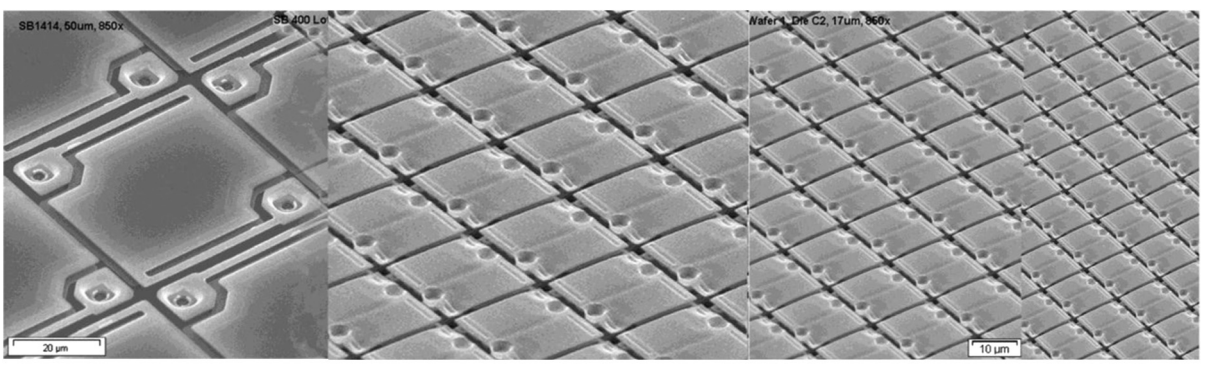

Fig. 5 Significant design and process challenges exist when a bolometer structure is reduced from 50 μm to a notional 12-μm design.

Downloaded From: http://spiedigitallibrary.org/ on 05/08/2013 Terms of Use: http://spiedl.org/terms

times the temperature fluctuation noise and all the other parameters now known, the problem reduces to the value of thermal conductance needed once the detector size is selected.

The design relations indicate that as the pixel gets smaller, the conductance must go down. This is because as the detector area decreases resulting in less signal power, the thermal conductance must decrease to maintain the same response. But as the pixel gets smaller, absent a change in design rules allowing legs with smaller cross sectional area, the legs get shorter and the thermal conductance increases. In the past, some designs made the legs longer by folding them underneath the pixel as the size went from 50 to 17 μm (Fig. 4). This allowed the legs to be thinner and/or narrower by separating the thermal isolation from the optical fill-factor. Reducing the pixel size from 17 to $\sim$10 μm and assuming the same total noise as twice the temperature fluctuation value, and maintaining the absorption efficiency and time constant, requires that the thermal conductance go from values near 10^{-8} W/K to 0.3×10^{-8} W/K. While there is no theoretical physics reason that stands in the way, other than some potential $1/f$ noise issues, the practical problem is whether a bolometer manufacturer possesses or has access to lithography tools at an acceptable cost to manufacture the bridges and legs to achieve such thermal isolation and accompanying thermal mass, and also to make denser read-out integrated circuits (ROIC). Often, the first resort is to push or stretch the capabilities of existing tools used to make a previous generation of detectors for making smaller designs, but that is usually at the cost of lower yields. Whether that is acceptable depends on the importance and benefits of the smaller design together with any savings of lower materials costs. Therefore the use of CMOS/MEMS (class1) commercial foundries is one way to take advantage of a huge process capability.

While there are reasons, as explained above, for not making uncooled pixel smaller than between 5 and 10 μm, depending on the particulars for long-wave infrared (LWIR) applications, there is room to make the detector more sensitive for several reasons. The first is that it allows a trade against *F*/number and Blur to maintain the system NETD (i.e., smaller optics). Second, it can be traded for shorter time constants while maintaining system NETD.

5 Approaching the Performance Limit

We can obtain a basic qualitative idea of the limit in performance subject to and in the context of some simplifying approximations, including absence of bias effects. We note that G is actually the sum of the thermal conductance of the legs G_l and g_r where g_r is the radiation conduction that remains when the legs hypothetically disappear. The radiation conductance arises from the first term of the expansion of Wien's law for radiating bodies. That is:

$$P_r = \varsigma \sigma A_D T_D^4 \quad \text{And thus } g_r = 4\varsigma\sigma A_D T_D^3,$$

where ς is a factor that accounts for emissivity of the detector and wavelength band if less than full blackbody and A_D is an effective area accounting for both sides and any reflective surfaces on the bolometer substrate. T_D is the detector temperature and is nominally 300 K, and σ is the Stefan-Boltzmann constant. In our simple case, the detector temperature about which the signal temperature fluctuates and substrate temperatures are the same. For simplicity, we assume that any shielding of the detector is at the same temperature as the ROIC on which the detector resides and that the average scene temperature is the same as the ROIC substrate. However, the expressions for P_r, g_r, and the parameter ς assume that the detector radiates in all directions including into any shielding as well as out the aperture into the scene. The parameter ς is one if we assume a perfect blackbody radiating over all wavelengths. Restricting the radiation to the pass band of the optics may reduce that to about 1/3. If we assume perfect reflectivity of the shielding and substrate so that the detector can only radiate out through the aperture and exchange heat energy with the scene, P_r and g_r may be written as

$$P_r = \frac{\varsigma \sigma A_D T_D^4}{4F^2 + 1} \quad \text{and} \quad g_r = \frac{4\varsigma\sigma A_D T_D^3}{4F^2 + 1}.$$

By explicitly writing the thermal conductance as the sum of leg and the radiation conductance and with slight rearrangement, we can write where N_i denotes noise terms other than temperature fluctuation:

$$\Delta T_{\mathrm{NeTD}} = \frac{(4F^2 + 1)G_l + 4\varsigma\sigma A_D T_{\mathrm{sub}}^3}{\eta A_D \frac{dP_b}{dT_b}} \times \sqrt{\frac{kT_{\mathrm{sub}}^2}{C_{\mathrm{th}}}} \sqrt{1 + (N_1^2 + N_2^2 + \dots)}.$$

Whereas we may desire to make G_l tend toward zero leaving only the radiation conductance to boost signal and reduce NETD, we also desire to keep the thermal time constant fixed to maintain the frame rate or information rate for the camera. The thermal time constant is

$$\tau = \frac{C_{\mathrm{th}}}{G_l + (4\varsigma\sigma A_D T_{\mathrm{sub}}^3)/(4F^2 + 1)}, \quad \text{or}$$

$$C_{\mathrm{th}} = \tau\left(G_l + \frac{4\varsigma\sigma A_D T_{\mathrm{sub}}^3}{4F^2 + 1}\right).$$

Thus we see that reducing the thermal conductance requires reducing the thermal mass. We note that reducing the thermal mass tends to increase the total temperature fluctuation exchange noise and reaches the maximum when G_l becomes zero. Replacing C_{th} in the first radical we obtain:

$$\Delta T_{\mathrm{NeTD}} = \frac{\sqrt{G_l + 4\varsigma\sigma A_D T_{\mathrm{sub}}^3/(4F^2 + 1)} \sqrt{\frac{kT_{\mathrm{sub}}^2}{\tau}} \sqrt{1 + (N_1^2 + N_2^2 + \dots)}}{\eta \frac{1}{4F^2+1} A_D \frac{dP_b}{dT_b}}.$$

Downloaded From: http://spiedigitallibrary.org/ on 05/08/2013 Terms of Use: http://spiedl.org/terms

In this simple description, the NETD can be reduced by taking $G_l \to 0$ or reducing the noise terms N_1, N_2 etc. or both. Reducing G_l to zero we obtain

$$\Delta T_{\mathrm{NeTD}} = \frac{\sqrt{\frac{4\varsigma\sigma k T_{\mathrm{sub}}^5 (4F^2+1)}{\tau}}\sqrt{1+(N_1^2+N_2^2+\ldots)}}{\eta\sqrt{A_D}\frac{dP_b}{dT_b}}.$$

We reach the ideal NETD when all noise sources are small except for the temperature fluctuation noise so that only the term 1 remains in the sum of noises. We obtain

$$\Delta T_{\mathrm{NeTD}} = \frac{1}{\eta(dP_b/dT_b)}\sqrt{\frac{4\varsigma\sigma k T_{\mathrm{sub}}^5 (4F^2+1)}{\tau A_D}}.$$

This last approximation may stretch the limits of the initial assumption that the bias power and its contributions are negligible.[10–12]

Assuming an 8- to 12-μm band, 100% efficiency, 300 K, 10-μm detectors, and ς to be somewhere around $1/3$, $F = 1$ and 10 ms time constant, we obtain an NETD ~1.5 mK. The radiation conductance is approximately 0.0044×10^{-8} W/K. To achieve that, we would need to have the detector levitate over the substrate and have a warm shield and substrate that does not interact with the detector. If we may assume a reflecting warm-shield that contributes about the same as the radiation conductance through the lens and 70% absorption efficiency, some leg conductance near the radiation limit to allow for electrical connections and three equal parts noise added to temperature fluctuation noise, we may get into the neighborhood of 7 or 8 mK. While state-of-the-art equipment exists to contemplate an attempt to make detectors with the required thermal conductance and accompanying thin bridges to maintain usable time constants, the demand for detectors approaching the radiation limit and the cost to realize such a device is not currently considered for uncooled products.

6 Summary and Conclusions

The trades between System MTF and smaller pixels allowing smaller die suggests that pixels sizes may be reduced to between 5 and 10 μm for uncooled LWIR applications. The benefits of doing so are smaller optics, smaller die and systems, and less weight and power assuming that performance metrics are maintained. In addition, smaller pixels provide more FPAs per wafer (lower cost/die) or permit larger formats at a reasonable cost. This may require better optics designs, since at such smaller pixels the optics MTF may become a limiting factor. It also requires uncooled detectors that have significant better sensitivity due to loss in signal as the size decreases, and will require better photolithography tools to manufacture the thin bridges and legs required to maintain sensitivity. This is mainly related to access or availability of such tools at a reasonable cost. Additionally, there is still considerable improvement possible as present uncooled bolometer detectors are still far from the fundamental limits of performance. Flexibility in system design suggests that pixel sizes smaller than 10 μm may be the practical limit for a focal plane that would be used for all applications.

References

1. C.-L. Tisse et al., "An information-theoretic perspective on the challenges and advances in the race towards 12 μm pixel pitch megapixel uncooled infrared imaging," *Proc. SPIE* **8353**, 83531M (2012).
2. S. Tohyama et al., "Uncooled infrared detectors toward smaller pixel pitch with newly proposed pixel structure," *Proc. SPIE* **8012**, 80121M (2011).
3. R. Morrison et al., "An alternative approach to infrared optics," *Proc. SPIE* **7660**, 76601Y (2010).
4. H. Driggers, "Small detector in infrared system design," *Opt. Eng.* **51**(9), 096401 (2012).
5. D. F. Murphy et al., "High sensitivity (25 μm pitch) microbolometer FPAs and applications development," *Proc. SPIE* **4369**, 222–234 (2001).
6. S. H. Black et al., "Advances in high rate uncooled detector fabrication at Raytheon," *Proc. SPIE* **7660**, 76600X (2010).
7. P. E. Howard et al., "DRS U6000 640×480 VOx uncooled IR focal plane," *Proc. SPIE* **4721**, 48–56 (2002).
8. P. Norton et al., "Uncooled thermal imaging sensor and application advances," *Proc. SPIE* **6206**, 620617 (2006).
9. D. F. Murphy et al., "High sensitivity 640×512 (20 μm pitch) microbolometer FPAs," *Proc. SPIE* **6206**, 62061A (2006).
10. R. A. Wood Chapter 3, "Uncooled infrared imaging arrays and systems," in *Semiconductors and Semimetals*, P. Kruse and D. Skatrud, Eds., pp. 43–90, Academic Press, San Diego, CA (1997).
11. P. W. Kruse, L. D. McGlauchlin, and R. B. McQuistan, Chapter 9, "Elements of Infrared Technology," in *Elements of Infrared Technology*, pp. 345–356, Wiley, New York (1962).
12. R. C. Jones, "The general theory of bolometer performance," *J. Opt. Soc. Am.* **43**(1), 102–115 (1953).

Biographies and photographs of the authors are not available.

Downloaded From: http://spiedigitallibrary.org/ on 05/08/2013 Terms of Use: http://spiedl.org/terms